

Disorder-Induced Mimicry of a Spin Liquid in YbMgGaO_4

Zhenyue Zhu,¹ P. A. Maksimov,¹ Steven R. White,¹ and A. L. Chernyshev¹

¹*Department of Physics and Astronomy, University of California, Irvine, California 92697, USA*

(Dated: October 16, 2018)

We suggest that a randomization of the pseudo-dipolar interaction in the spin-orbit-generated low-energy Hamiltonian of YbMgGaO_4 due to an inhomogeneous charge environment from a natural mixing of Mg^{2+} and Ga^{3+} can give rise to orientational spin disorder and mimic a spin-liquid-like state. In the absence of such quenched disorder, $1/S$ and density matrix renormalization group calculations both show robust ordered states for the physically relevant phases of the model. Our scenario is consistent with the available experimental data and further experiments are proposed to support it.

PACS numbers: 75.10.Jm, 75.40.Gb, 78.70.Nx

Dating back to Wannier's pioneering study of the Ising model [1], triangular lattice models and materials with frustrating antiferromagnetic interactions have served as fertile playgrounds for new ideas [2–10]. These systems continue to draw significant experimental [11–15] and theoretical interest because they exhibit many intriguing novel ordered states [16–22] and unusual continuum-like spectral features [23–31] and especially because they provide a setting for spin-liquid states [32–42].

Among the latest experimental discoveries [14, 15], a rare-earth triangular-lattice antiferromagnet YbMgGaO_4 has recently emerged as a new candidate for a quantum spin liquid of the effective spin-1/2 degrees of freedom of Yb^{3+} ions [43, 44]. It has been argued that the spin-orbit origin of its magnetic properties and the pseudo-spin nature of the low-energy states with highly anisotropic effective spin interactions may potentially open a new route to realizing quantum spin liquids [44–46]. While the lack of ordering, anomalous specific heat, and especially continuum-like excitations in inelastic neutron scattering [45, 47] all provide strong support to the idea of an intrinsic spin liquid, other experimental findings are increasingly at odds with this picture.

First, in magnetization vs field measurements, there is no sharpening of the transition to the saturated phase upon lowering the temperature, and the lack of the upward curvature in $M(H)$ at the lowest T 's [43, 44] is indicative of low quantum fluctuations in the ground state [48]. Second, in the high-field polarized phase, neutron scattering shows that continuum-like excitations persist, with significant smearing of magnon lines that are expected to be sharp [47]. In addition, an apparent absence of any detectable contribution of spin excitations to thermal conductivity down to the lowest temperatures, accompanied by a strong deviation of the phonon part from the ballistic T^3 form [49], both suggest strong scattering effects. These, combined with the anomalously broadened higher-energy Yb^{3+} doublet structure [47, 50] and a ubiquitous mixing of Mg^{2+} and Ga^{3+} ions in the non-magnetic layers [43, 47], implicate disorder as a key contributor to the observed properties [50].

In this Letter, we first argue that a hypothetical, disorder-free version of YbMgGaO_4 should exhibit a robust collinear/stripe magnetic order. We demonstrate this by extending the well-studied phase diagram of the triangular-lattice Heisenberg $J_1 - J_2$ model, which is known to have an extensive spin-liquid region for $S = 1/2$ [33–40], to the anisotropic version of the model that corresponds to the types of anisotropy allowed in YbMgGaO_4 with realistic restrictions from experiments. A significant XXZ anisotropy present in YbMgGaO_4 suppresses the spin-liquid region of the phase diagram, and the pseudo-dipolar interactions further diminish it. Both types of anisotropy lower the symmetry and produce gaps in the excitation spectra, reducing quantum fluctuations that suppress the ordered states.

We then suggest that the stripe order is fragile to an orientational disorder that can be easily produced via a randomization of the subleading pseudo-dipolar interactions. The physical reason of such a sensitivity is a small energetic barrier, $\delta E \sim 0.03J_1$ per site, between the stripe phases of different spatial orientations, which, in the absence of the pseudo-dipolar terms, are selected by order-by-disorder fluctuations. Thus, we propose that the spin-liquid-like state in YbMgGaO_4 is disorder induced and is composed of nearly classical, orientationally randomized, short-range stripe-like spin domains. The quenched, spatially-fluctuating charge environment of the magnetic Yb^{3+} ions due to random site occupancies of Mg^{2+} and Ga^{3+} ions is seen as a likely culprit, affecting the low-energy effective spin Hamiltonian through the spin-orbit coupling.

Model.—Although the magnetism of YbMgGaO_4 is dominated by spin-orbit coupling, which can result in large spin anisotropies of various types [51–54], it is restricted by the high symmetry of the lattice [44, 45], yielding the familiar XXZ anisotropy accompanied by the so-called pseudo-dipolar terms. Moreover, the local character of the f shells on Yb dictates that the dominant interactions are between the nearest-neighbor spins, further restricting possible spin models.

Thus, we are compelled to explore the phase diagram

of the following $S=1/2$ model as relevant to YbMgGaO_4 [43–45, 47] and also to a broader family of the rare-earth triangular-lattice materials [55]: $\mathcal{H} = \mathcal{H}_{XXZ}^{J_1-J_2} + \mathcal{H}_{\text{pd}}$, with

$$\mathcal{H}_{XXZ}^{J_1-J_2} = \sum_{\langle ij \rangle_n} J_n (S_i^x S_j^x + S_i^y S_j^y + \Delta S_i^z S_j^z), \quad (1)$$

where the sums are over the (next-)nearest neighbors with $J_1 > J_2 \geq 0$, the XXZ anisotropy $0 \leq \Delta \leq 1$, and the pseudo-dipolar terms introduced as [44, 45, 47]

$$\mathcal{H}_{\text{pd}} = J_{\pm\pm} \sum_{\langle ij \rangle} (e^{i\tilde{\varphi}_\alpha} S_i^+ S_j^+ + e^{-i\tilde{\varphi}_\alpha} S_i^- S_j^-), \quad (2)$$

where $S^\pm = S^x \pm iS^y$ and $\tilde{\varphi}_\alpha = \{0, -2\pi/3, 2\pi/3\}$ are the bond-dependent phases for the primitive vectors δ_α , with δ_α 's and x and y axes as in Fig. 1(a). Although this is not obvious from (2) [56], the pseudo-dipolar terms favor the direction of the spins on a bond to be either parallel or perpendicular to the bond [52]. Because of the high symmetry of the lattice, the Dzyaloshinsky-Moriya interactions are forbidden [43, 57] and we also omit the couplings of $S^{x(y)}$'s to the out-of-plane S^z 's, referred to as the $J_{z\pm}$ terms, as they are negligible in YbMgGaO_4 [44, 47] and do not affect our conclusions. An intuitive derivation of the Hamiltonian is given in [58].

XXZ only.—In YbMgGaO_4 , electron spin resonance (ESR), magnetic susceptibility, and neutron scattering [44, 47] have suggested strong XXZ anisotropy, $\Delta \sim 0.5$, and put rather stringent bounds on the pseudo-dipolar terms, indicating their subleading role. Thus, we study the pure XXZ model (1) first, considering effects of the pseudo-dipolar terms next. The anisotropy for J_1 and J_2 bonds, Δ_1 and Δ_2 , is assumed equal [47], as it originates from the magnetic state of Yb^{3+} ions, with no qualitative changes expected for $\Delta_1 \neq \Delta_2$.

While the Heisenberg version of (1) at $\Delta=1$ is well explored [33–40], its anisotropic extension has been studied only rarely [59, 60]. For $J_2/J_1 < 1$, two ordered states compete, the 120° and the collinear state, where in the latter ferromagnetic rows (“stripes”) of spins align antiferromagnetically; see Fig. 1(a). Their classical energies are $E_{\text{gs}}^{120^\circ} = -3(J_1/2 - J_2)$ and $E_{\text{gs}}^{\text{str}} = -J_1 - J_2$ (per NS^2), yielding a transition at $J_2 = J_1/8$ [34, 35] independent of Δ . It is important to note that XXZ anisotropy leads to an overlap of the J_2 ranges of stability for magnon spectra of the competing phases [58, 59]. This implies that the spin-wave instabilities do not yield an intermediate magnetically disordered state for $S \gg 1$, favoring instead a direct transition between the two orders.

The $J_2 - \Delta$ phase diagram of $\mathcal{H}_{XXZ}^{J_1-J_2}$ for $S=1/2$, obtained via the spin-wave theory (SWT) and density matrix renormalization group (DMRG) calculations, is shown in Fig. 1(b). The color map shows the ordered moment $\langle S \rangle$ and the $\langle S \rangle = 0$ boundaries of a non-magnetic phase (gray) according to the SWT. The solid black line marks the crossing of $\langle S \rangle$ from the 120° to the stripe

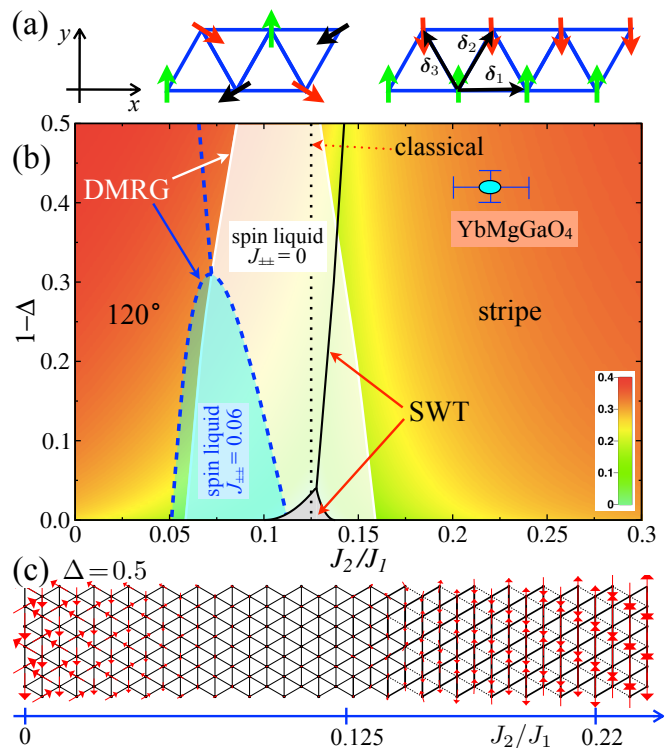


FIG. 1: (a) Axes, primitive vectors, and a sketch of the 120° and stripe states. (b) $1-\Delta$ vs J_2 phase diagram of the XXZ model (1). The $\langle S \rangle$ color map and boundaries (solid lines) are by the SWT; the dotted line is the classical phase boundary. The shaded white area is the spin-liquid region by the DMRG; see the text. The dashed line with the shaded region is the same for the model with \mathcal{H}_{pd} with $|J_{\pm\pm}| = 0.06$; see Fig. 2. The error bars mark YbMgGaO_4 parameters from Ref. [47]. (c) The DMRG scan of (1) vs J_2 for $\Delta=0.5$ with up to 2000 states.

phase. It outlines a region where the SWT predicts a direct transition with no intermediate state. Note that the SWT ground state energies indicate this transition to be on the left of the classical $J_2 = J_1/8$ line for $\Delta < 1$ [58].

Figure 1(c) shows a DMRG calculation of the model (1) for $\Delta=0.5$ where J_2 is varied along the length of the cylinder so that different phases appear at different regions. The orders are pinned at the boundaries and the spin patterns give a faithful visual extent of their phases. Similar scans for several Δ 's allow us to map out the phase diagram of the model [33, 61]. To roughly estimate the J_2 boundaries for the spin liquid (SL), we use the cutoff value of $\langle S \rangle = 0.05$, below which the system is assumed to be in a SL state. This procedure matches the SL boundaries for the isotropic ($\Delta=1$) $J_1 - J_2$ model found in Ref. [33] by a more accurate method. The resultant extent of the SL phase is shown in Fig. 1(b) by the white shaded area. We note that the $\langle S \rangle$ cutoff value that we use may overestimate the SL region at $\Delta < 1$, as the anisotropy tends to stabilize ordered phases, while the SWT clearly underestimates it, as expected.

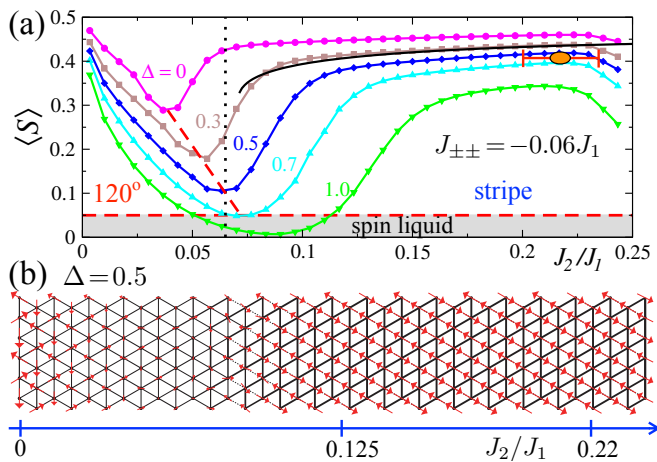


FIG. 2: (a) DMRG results for $\langle S \rangle$ vs J_2 with $|J_{\pm\pm}| = 0.06J_1$. Dotted and dashed lines denote classical and DMRG phase boundaries, respectively. The error bar is the same as in Fig. 1(b). The solid black line is the SWT result for $\Delta = 0.5$. (b) A long-cylinder DMRG scan for $\Delta = 0.5$ and $J_{\pm\pm} = -0.06J_1$.

The ellipse with error bars in Fig. 1(b) marks $J_2/J_1 = 0.22(2)$ and $\Delta = 0.58(2)$, proposed for YbMgGaO_4 [47]. For these parameters (with $J_{\pm\pm} = 0$), we find a close agreement between the DMRG and SWT on the ordered moment, 0.29 and 0.32, respectively, implying that YbMgGaO_4 is deep in the stripe phase.

Pseudo-dipolar terms.—The anisotropic terms in (2) explicitly break the U(1) symmetry of the XXZ model (1) and are expected to pin the spin directions to the lattice. This is indeed true for the stripe phase, in which the pseudo-dipolar terms make the spin orientation parallel ($J_{\pm\pm} < 0$) or perpendicular ($J_{\pm\pm} > 0$) to the stripe direction [58] as in Figs. 2(b) or 1(a); see also [57]. From the $1/S$ perspective, no pinning and no change of the classical energy occurs due to (2) for the 120° phase, which, however, remains stable [58]. On the other hand, the partially frustrated pseudo-dipolar terms in (2) lower the classical energy of the stripe phase by $-4|J_{\pm\pm}|S^2N$ and expand its stability range by shifting the classical phase boundary to a lower $J_2 = J_1/8 - |J_{\pm\pm}|$.

In Figs. 2 and 1(b), we show the effect of adding $J_{\pm\pm}$ to the model, using $|J_{\pm\pm}| = 0.06J_1$, as suggested by ESR [44]. The classical transition between the 120° and stripe phases is at $J_2 = 0.065J_1$ for this value of $|J_{\pm\pm}|$, with the DMRG long-cylinder scans showing it tilting toward smaller J_2 at smaller Δ . Using the same generous criteria for the spin liquid as above, the DMRG results show that $J_{\pm\pm}$ shrinks the SL region [light blue in Fig. 1(b)], and moves it farther from the YbMgGaO_4 parameters. It also strengthens the stripe order [Fig. 2(a)], in close agreement with the SWT (solid line). The agreement for the ordered moment for YbMgGaO_4 parameters [47] is very close, $\langle S \rangle \approx 0.419$ (0.433) by DMRG (SWT), and the magnitude of the order parameter is large.

Thus, in this model for YbMgGaO_4 , the easy-plane

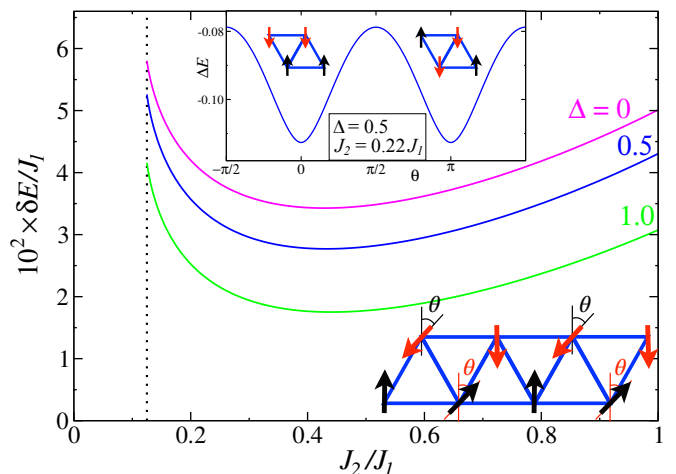


FIG. 3: Energy barrier between the stripe states of different orientations in the XXZ J_1 – J_2 model vs J_2 for various Δ and $S = 1/2$. Upper inset: Quantum energy correction vs angle θ . Lower inset: A sketch of the degenerate classical ground states with $\theta = 0(\pi)$ corresponding to two stripe orientations.

and pseudo-dipolar anisotropies both lead to a stronger stripe order. Yet, the experiments show no sign of it.

Alternative sets of parameters with much larger values of $|J_{\pm\pm}| = 0.26J_1$ [62] and $0.69J_1$ [47] were obtained by fitting the high-field magnon dispersion in YbMgGaO_4 [47] without the J_2 term in (1). Both values strongly deviate from the ESR data [44] and imply an almost classical stripe state with nearly saturated ordered moments and large magnon gaps [58], inconsistent with the observed substantial spectral weight at low energies [47]. For $|J_{\pm\pm}| \gtrsim 0.2$, there is no 120° state left in the phase diagram to compete with, leaving no SL state in sight.

Barrier.—Before we attempt to reconcile our finding of strong stripe order in the model with the lack of order in YbMgGaO_4 , we give the J_1 – J_2 XXZ model (1) a second look. Classically, in the absence of the pseudo-dipolar terms, the stripe phases of Fig. 1(a) are degenerate with a manifold of spiral phases in Fig. 3, in which four spins in the two side-sharing triangles add up to zero [34, 35]. Their degeneracy is lifted via order-by-disorder mechanism [63, 64], selecting the three stripe states that break rotational lattice symmetry. The tunneling barrier between them, $\delta E(J_2, \Delta)/N$, shown in Fig. 3, is obtained from the quantum energy correction $\Delta E(\theta) = c + \frac{1}{2} \sum_{\mathbf{k}} \varepsilon_{\mathbf{k}}(\theta)$, where $c = -(J_1 + J_2)S$ and $\varepsilon_{\mathbf{k}}(\theta)$ is the magnon energy, which depends on the angle θ of the spiral state from the degenerate classical manifold. As one can see from Fig. 3, the tunneling barrier is small, $\delta E \sim 0.03J$ per site, similar to the J_1 – J_2 model on the square lattice [65]. Thus, in the XXZ model, despite being strongly ordered, the stripe phases of different orientations are separated by a low energetic barrier.

Disorder.—As discussed above, a number of experiments indicate a substantial disorder in the low-energy effective spin Hamiltonian of YbMgGaO_4 [43, 47, 49, 50]. Most direct are the neutron studies, suggesting strong

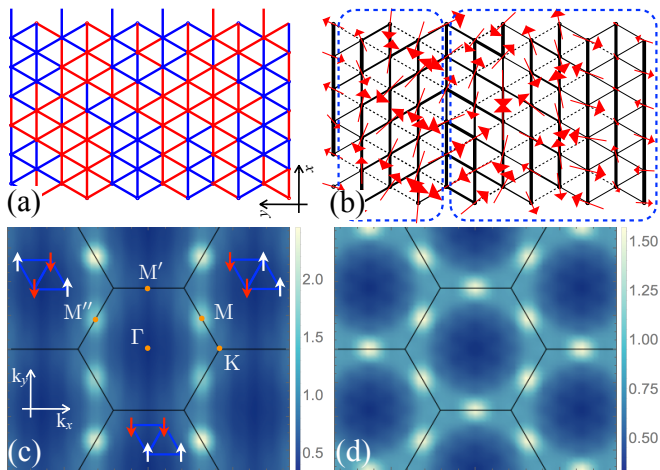


FIG. 4: (a) Positive and negative $J_{\pm\pm}$ bonds in a typical disorder realization. (b) Two stripe domains (dashed boxes) for random $|J_{\pm\pm}| = 0.2J_1$, $\langle S \rangle$ up to 0.33. (c) $S(\mathbf{q})$ [66] for random $|J_{\pm\pm}| = 0.1(0.05)J_1$. (d) Averaged $S(\mathbf{q})$ from (c); see the text.

variations in the effective g factors and, possibly, magnetic couplings [50] due to a random charge environment from mixing of the non-magnetic Mg^{2+} and Ga^{3+} .

We do not attempt to analyze all forms of disorder that can naturally occur in the Hamiltonian (1) and (2). Instead, we propose that a disorder in the $J_{\pm\pm}$ terms should be potentially very destructive. Because of their pseudo-dipolar nature, random $J_{\pm\pm}$'s are not unlike fluctuating pinning fields that can locally stabilize stripes with different orientations by overcoming the low tunneling barrier between them. In addition, for the relevant values of $|J_{\pm\pm}| \sim 0.1J_1 \gtrsim \delta E$, fluctuations of the diagonal elements of the exchange tensor at the level of $0.1 - 0.2J_1$, that are consistent with the variations suggested in Ref. [50], translate into completely random $J_{\pm\pm}$ [58].

We have performed DMRG calculations of the $J_1 - J_2$ XXZ model (1) with YbMgGaO_4 parameters, $\Delta = 0.58$ and $J_2 = 0.22J_1$ [47], and random $J_{\pm\pm}$ (2). We have used different random disorder realizations, such as in Fig. 4(a), with a binary distribution of $J_{\pm\pm}$ of alternating sign and a global constraint of the same number of positive and negative $J_{\pm\pm}$ bonds to reduce the finite-size bias. We used the values of $|J_{\pm\pm}|/J_1 = 0.05, 0.1$, and 0.2 on the 6×12 cluster. The results are as follows.

For large values of random $|J_{\pm\pm}| = 0.2J_1$, the ground states tend to contain static, visibly disordered spin domains with mixed stripe orientations and large ordered moments; see Fig. 4(b). For smaller $|J_{\pm\pm}|$, more interesting states appear. First, there is no clear real-space order without pinning fields, as in a disorder-free $U(1)$ -symmetric XXZ model, yet the structure factor [66], obtained from $S_{\mathbf{q}}^{\alpha\beta} = \sum_{i,j} \langle S_i^\alpha S_j^\beta \rangle e^{i\mathbf{q}(\mathbf{R}_i - \mathbf{R}_j)}$, shows broadened peaks at *two* M points, which are associated with *two different* stripe orderings; see Fig. 4(c). We note that the 6×12 DMRG cluster strongly disfavors the state with

stripes along the shorter direction of the cylinder, parallel to the open boundaries, that would show itself as a peak at the M' points in Fig. 4(c).

Upon a careful investigation with pinning fields, we conclude that the observed state is a *stripe-superposition state*, in which spins continue to fluctuate collectively between the two stripe states allowed by the cluster. A hint of such a state can also be seen at the right edge in Fig. 4(b). As opposed to a spin liquid, the degeneracy of such a superposed state is not extensive. This finding implies that the randomization of $J_{\pm\pm}$ leads to an effective restoration of the Z_3 lattice symmetry, broken in each individual stripe state. Whether such stripe-superposition states will be pinned to form single-stripe domains on a larger length scale, or they will survive as localized fluctuating states, remains an open question.

Note that both $|J_{\pm\pm}|/J_1 = 0.05$ and 0.1 yield nearly identical structure factors, with the smaller value already sufficient to destroy the long-range stripe order, supporting our hypothesis on its fragility to an orientational disorder. To overcome the lack of the third stripe direction in the DMRG cluster and provide a faithful view of a response of a spatially isotropic system, we have performed an averaging of the structure factor [see Fig. 4(d)], with the results very similar to the $S(\mathbf{q})$ in the neutron-scattering data for YbMgGaO_4 [47].

Altogether, the randomization of the small pseudo-dipolar term in the model description of YbMgGaO_4 results in the disordered stripe ground states that can successfully mimic a spin liquid. Further experimental verifications of the proposed picture include possible freezing at lower temperatures, as the current lowest-temperature measurements [47] are at $T \sim 0.05J_1 \sim |J_{\pm\pm}|$, and the spin pseudo-gap in the dynamical response at low energies at the M points as a remnant of the anisotropy-induced gaps in the magnon spectra [58]. The proposed scenario implies that the anomalously low T power in the specific heat should emerge as a result of disorder.

Summary.—We have investigated a generalization of the isotropic $J_1 - J_2$ triangular-lattice model, known to support a spin-liquid state, and have found that the anisotropic interactions significantly diminish the spin-liquid region of the phase diagram. Our analysis finds no additional transitions near the experimentally relevant range of parameters, putting YbMgGaO_4 firmly in the stripe-ordered state. At the same time, the stripe states are shown to be fragile toward orientational disorder. The randomization of the pseudo-dipolar interactions due to the spatially fluctuating charge environment of the magnetic ions generates a mimicry of a spin-liquid state in the form of short-range stripe or stripe-superposition domains. This scenario is likely to be relevant to other rare-earth-based quantum magnets.

We thank Andrey Chubukov and Natalia Perkins for fruitful conversations, Mike Zhitomirsky and Sid Parameswaran for pointed comments, Oleg Starykh for

patient explanations and helpful feedback, and Kate Ross for an enlightening discussion. We are immensely grateful to Ioanis Rousochatzakis for sharing his old notes on the order-by-disorder effect and for many valuable remarks. We are particularly indebted to Martin Mourigal for his indispensable comments, numerous conversations, constructive attitude, and extremely useful insights. This work was supported by the U.S. Department of Energy, Office of Science, Basic Energy Sciences under Award No. DE-FG02-04ER46174 (P. A. M. and A. L. C.) and by the NSF through Grant DMR-1505406 (Z. Z. and S. R. W.). A. L. C. thanks Aspen Center for Physics, where part of this work was done. The work at Aspen was supported in part by NSF Grant No. PHYS-1066293.

Note added. Recently, we became aware of work that supports our findings [67].

-
- [1] G. H. Wannier, Phys. Rev. **79**, 357 (1950).
 [2] P. W. Anderson, Mater. Res. Bull. **8**, 153 (1973); P. Fazekas and P. W. Anderson, Philos. Mag. **30**, 423 (1974).
 [3] D. A. Huse and V. Elser, Phys. Rev. Lett. **60**, 2531 (1988).
 [4] T. Oguchi, J. Phys. Soc. Jpn. Suppl. **52**, 183 (1983); Th. Jolicoeur and J. C. Le Guillou, Phys. Rev. B **40**, 2727 (1989).
 [5] S. J. Miyake, J. Phys. Soc. Jpn. **61**, 983 (1992).
 [6] A. V. Chubukov, S. Sachdev, and T. Senthil, J. Phys. Condens. Matter **6**, 8891 (1994).
 [7] P. W. Leung and K. J. Runge, Phys. Rev. B **47**, 5861 (1993).
 [8] B. Bernu, P. Lecheminant, C. Lhuillier, and L. Pierre, Phys. Rev. B **50**, 10048 (1994).
 [9] L. Capriotti, A. E. Trumper, and S. Sorella, Phys. Rev. Lett. **82**, 3899 (1999).
 [10] S. R. White and A. L. Chernyshev, Phys. Rev. Lett. **99**, 127004 (2007).
 [11] M. F. Collins and O. A. Petrenko, Can. J. Phys. **75**, 605 (1997).
 [12] S. Nakatsuji, Y. Nambu, H. Tonomura, O. Sakai, S. Jonas, C. Broholm, H. Tsunetsugu, Y. Qiu, and Y. Maeno, Science **309**, 1697 (2005).
 [13] A. Olariu, P. Mendels, F. Bert, B. G. Ueland, P. Schiffer, R. F. Berger, and R. J. Cava, Phys. Rev. Lett. **97**, 167203 (2006).
 [14] H. D. Zhou, C. Xu, A. M. Hallas, H. J. Silverstein, C. R. Wiebe, I. Umegaki, J. Q. Yan, T. P. Murphy, J.-H. Park, Y. Qiu, J. R. D. Copley, J. S. Gardner, and Y. Takano, Phys. Rev. Lett. **109**, 267206 (2012).
 [15] R. Rawl, L. Ge, H. Agrawal, Y. Kamiya, C. R. Dela Cruz, N. P. Butch, X. F. Sun, M. Lee, E. S. Choi, J. Oitmaa, C. D. Batista, M. Mourigal, H. D. Zhou, and J. Ma, Phys. Rev. B **95**, 060412 (2017).
 [16] H. Kawamura and S. Miyashita, J. Phys. Soc. Jpn. **54**, 4530 (1985).
 [17] S. E. Korshunov, J. Phys. C **19**, 5927 (1986).
 [18] A. V. Chubukov and D. I. Golosov, J. Phys. Condens. Matter **3**, 69 (1991).
 [19] D. Yamamoto, G. Marmorini, and I. Danshita, Phys. Rev. Lett. **112**, 127203 (2014).
 [20] O. A. Starykh, W. Jin, and A. V. Chubukov, Phys. Rev. Lett. **113**, 087204 (2014).
 [21] D. Sellmann, X.-F. Zhang, and S. Eggert, Phys. Rev. B **91**, 081104 (2015).
 [22] O. A. Starykh, Rep. Prog. Phys. **78**, 052502 (2015).
 [23] R. Coldea, D. A. Tennant, A. M. Tsvelik, and Z. Tylczynski, Phys. Rev. Lett. **86**, 1335 (2001).
 [24] W. Zheng, J. O. Fjærestad, R. R. P. Singh, R. H. McKenzie, and R. Coldea, Phys. Rev. B **74**, 224420 (2006).
 [25] O. A. Starykh, H. Katsura, and L. Balents, Phys. Rev. B **82**, 014421 (2010).
 [26] J. Ma, Y. Kamiya, T. Hong, H. B. Cao, G. Ehlers, W. Tian, C. D. Batista, Z. L. Dun, H. D. Zhou, and M. Matsuda, Phys. Rev. Lett. **116**, 087201 (2016).
 [27] J. Oh, M. D. Le, J. Jeong, J. H. Lee, H. Woo, W.-Y. Song, T. G. Perring, W. J. L. Buyers, S.-W. Cheong, and J.-G. Park, Phys. Rev. Lett. **111**, 257202 (2013).
 [28] M. E. Zhitomirsky and A. L. Chernyshev, Rev. Mod. Phys. **85**, 219 (2013).
 [29] O. A. Starykh, A. V. Chubukov, and A. G. Abanov, Phys. Rev. B **74**, 180403 (2006).
 [30] A. L. Chernyshev and M. E. Zhitomirsky, Phys. Rev. Lett. **97**, 207202 (2006); Phys. Rev. B **79**, 144416 (2009).
 [31] M. Mourigal, W. T. Fuhrman, A. L. Chernyshev, and M. E. Zhitomirsky, Phys. Rev. B **88**, 094407 (2013).
 [32] R. V. Mishmash, J. R. Garrison, S. Bieri, and C. Xu, Phys. Rev. Lett. **111**, 157203 (2013).
 [33] Z. Zhu and S. R. White, Phys. Rev. B **92**, 041105 (2015).
 [34] A. V. Chubukov and Th. Jolicoeur, Phys. Rev. B **46**, 11137 (1992).
 [35] Th. Jolicoeur, E. Dagotto, E. Gagliano, and S. Bacci, Phys. Rev. B **42**, 4800(R) (1990).
 [36] Y. Iqbal, W.-J. Hu, R. Thomale, D. Poilblanc, and F. Becca, Phys. Rev. B **93**, 144411 (2016).
 [37] R. F. Bishop and P. H. Y. Li, Europhys. Lett. **112**, 67002 (2015); P. H. Y. Li, R. F. Bishop, and C. E. Campbell, Phys. Rev. B **91**, 014426 (2015).
 [38] R. Kaneko, S. Morita, and M. Imada, J. Phys. Soc. Jpn. **83**, 093707 (2014).
 [39] C. J. Gazza, and H. A. Ceccatto, J. Phys. Condens. Matter **5**, L135 (1993).
 [40] R. Deutscher and H. U. Everts, Z. Phys. B **93**, 77 (1993).
 [41] R. Moessner and S. L. Sondhi, Phys. Rev. Lett. **86**, 1881 (2001).
 [42] L. Savary and L. Balents, Rep. Prog. Phys. **80**, 016502 (2017).
 [43] Y. Li, H. Liao, Z. Zhang, S. Li, F. Jin, L. Ling, L. Zhang, Y. Zou, L. Pi, Z. Yang, J. Wang, Z. Wu, and Q. Zhang, Sci. Rep. **5**, 16419 (2015).
 [44] Y. Li, G. Chen, W. Tong, Li Pi, J. Liu, Z. Yang, X. Wang, and Q. Zhang. Phys. Rev. Lett. **115**, 167203 (2015).
 [45] Y. Shen, Y.-D. Li, H. Wo, Y. Li, S. Shen, B. Pan, Q. Wang, H. C. Walker, P. Steffens, M. Boehm, Y. Hao, D. L. Quintero-Castro, L. W. Harriger, M. D. Frontzek, L. Hao, S. Meng, Q. Zhang, G. Chen, and J. Zhao, Nature (London) **540**, 559 (2016).
 [46] Y. S. Li, D. Adroja, P. K. Biswas, P. J. Baker, Q. Zhang, J. J. Liu, A. A. Tsirlin, P. Gegenwart, and Q. M. Zhang, Phys. Rev. Lett. **117**, 097201 (2016).
 [47] J. A. M. Paddison, M. Daum, Z. Dun, G. Ehlers, Y. Liu, M. B. Stone, H. Zhou, and M. Mourigal, Nat. Phys. **13**, 117 (2017).
 [48] R. B. Griffiths, Phys. Rev. **133**, A768 (1964).

- [49] Y. Xu, J. Zhang, Y. S. Li, Y. J. Yu, X. C. Hong, Q. M. Zhang, and S. Y. Li, Phys. Rev. Lett. **117**, 267202 (2016).
- [50] Y. Li, D. Adroja, R. I. Bewley, D. Voneshen, A. A. Tsirlin, P. Gegenwart, and Q. Zhang, Phys. Rev. Lett. **118**, 107202 (2017).
- [51] H. Yan, O. Benton, L. D. C. Jaubert, and N. Shannon, Phys. Rev. B **95**, 094422 (2017).
- [52] M. E. Zhitomirsky, M. V. Gvozdikova, P. C. W. Holdsworth, and R. Moessner, Phys. Rev. Lett. **109**, 077204 (2012).
- [53] K. A. Ross, L. Savary, B. D. Gaulin, and L. Balents, Phys. Rev. X **1**, 021002 (2011).
- [54] L. Savary, K. A. Ross, B. D. Gaulin, J. P. C. Ruff, and L. Balents, Phys. Rev. Lett. **109**, 167201 (2012).
- [55] M. B. Sanders, F. A. Cevallos, and R. J. Cava, Mater. Res. Express **4**, 036102 (2017).
- [56] For a more humane form of (2), see [58].
- [57] Y.-D. Li, X. Wang, and G. Chen, Phys. Rev. B **94**, 035107 (2016).
- [58] See Supplemental Material at <http://link.aps.org/supplemental/>, for the technical details, such as Hamiltonian derivation, additional SWT and DMRG results, polarized phase consideration, etc.
- [59] N. B. Ivanov, Phys. Rev. B **47**, 9105 (1993).
- [60] A. S. T. Pires, Physica (Amsterdam) A **391**, 5433 (2012).
- [61] Z. Zhu, D. A. Huse, and S. R. White, Phys. Rev. Lett. **110**, 127205 (2013); **111**, 257201 (2013).
- [62] Y.-D. Li, Y. Shen, Y. Li, J. Zhao, and G. Chen, arXiv:1608.06445.
- [63] P. Chandra, P. Coleman, and A. I. Larkin, Phys. Rev. Lett. **64**, 88 (1990).
- [64] C. L. Henley, Phys. Rev. Lett. **62**, 2056 (1989).
- [65] I. Rousochatzakis (private communication).
- [66] $\mathcal{S}(\mathbf{q}) = \sum_{\alpha\beta} (\delta_{\alpha\beta} - q_{\alpha}q_{\beta}/q^2) \mathcal{S}_{\mathbf{q}}^{\alpha\beta}$ is taken at $q_z = 0$.
- [67] Q. Luo, S. Hu, B. Xi, J. Zhao, and X. Wang, Phys. Rev. B **95**, 165110 (2017).

Disorder-induced mimicry of a spin liquid in YbMgGaO₄: Supplemental Material

Z. Zhu,¹ P. A. Maksimov,¹ S. R. White,¹ and A. L. Chernyshev¹

¹*Department of Physics and Astronomy, University of California, Irvine, California 92697, USA*

(Dated: June 9, 2017)

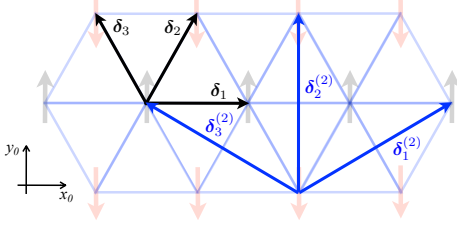


FIG. 1: Nearest and next-nearest primitive vectors.

Due to YbMgGaO₄ [1–4], easy-plane XXZ $J_1 - J_2$ antiferromagnetic model on a triangular lattice with additional anisotropic pseudo-dipolar spin-spin interactions is of recent interest. We discuss the phase diagram of this model and some aspects of its dynamical response using SWT approximation and DMRG.

Intuitive derivation of the Hamiltonian

Consider the most general form of the two-site spin-spin interaction on the δ_1 bond in Fig. 1 with $x_0 \parallel \delta_1$

$$\hat{H}_{12} = \mathbf{S}_1^0 \begin{pmatrix} J_{xx} & J_{xy} & J_{xz} \\ J_{yx} & J_{yy} & J_{yz} \\ J_{zx} & J_{zy} & J_{zz} \end{pmatrix} \mathbf{S}_2^0, \quad (1)$$

where $\mathbf{S}^0 = (S^{x_0}, S^{y_0}, S^{z_0})$. The 180° rotation around the δ_1 bond changes $y_0 \rightarrow -y_0$, $z_0 \rightarrow -z_0$, but should leave the two-site form (1) invariant, leaving us with

$$\hat{H}_{12} = \mathbf{S}_1^0 \begin{pmatrix} J_{xx} & 0 & 0 \\ 0 & J_{yy} & J_{yz} \\ 0 & J_{zy} & J_{zz} \end{pmatrix} \mathbf{S}_2^0. \quad (2)$$

Inversion with respect to the bond center and changing $1 \leftrightarrow 2$ should also leave (2) invariant, allowing only symmetric off-diagonal term, $J_{zy} = J_{yz}$. Renaming it $J_{z\pm} = J_{z\pm}$, and rewriting the diagonal terms using $J_{zz} = \Delta \cdot J_1$,

$$J_1 = (J_{xx} + J_{yy})/2, \quad J_{\pm\pm} = (J_{xx} - J_{yy})/4, \quad (3)$$

yields the two-site Hamiltonian for δ_1

$$\hat{H}_{12} = J_1 \left(\Delta S_1^{z_0} S_2^{z_0} + S_1^{x_0} S_2^{x_0} + S_1^{y_0} S_2^{y_0} \right) + 2J_{\pm\pm} \left(S_1^{x_0} S_2^{x_0} - S_1^{y_0} S_2^{y_0} \right) + J_{z\pm} \left(S_1^{z_0} S_2^{y_0} + S_1^{y_0} S_2^{z_0} \right), \quad (4)$$

which clearly follows the structure in Refs. [2, 3]. The first term is in the familiar XXZ form and the other two are referred to as pseudo-dipolar terms as they favor spin directions to be (anti)pinned to the bond direction [5].

For the other bonds, and for simplicity, we drop the $J_{z\pm}$ term as it will be ignored later and consider only the

in-plane spin components S^{x_0} and S^{y_0} . Using the invariance to a $\pi/3$ rotation around the z_0 axis to transform (2) to the δ_2 bond in Fig. 1, changes \hat{J}_1 matrix in (2) to

$$\hat{J}_2 = \mathbf{R}_{\pi/3}^{-1} \hat{J}_1 \mathbf{R}_{\pi/3}, \quad \mathbf{R}_\theta = \begin{pmatrix} \cos \theta & \sin \theta \\ -\sin \theta & \cos \theta \end{pmatrix}, \quad (5)$$

or, explicitly, for the two-component spins using (3)

$$\hat{J}_2 = \begin{pmatrix} J_1 + 2J_{\pm\pm} \cos \frac{2\pi}{3} & 2J_{\pm\pm} \sin \frac{2\pi}{3} \\ 2J_{\pm\pm} \sin \frac{2\pi}{3} & J_1 - 2J_{\pm\pm} \cos \frac{2\pi}{3} \end{pmatrix}. \quad (6)$$

For the bond δ_3 in Fig. 1, rotation is by $2\pi/3$ and

$$\hat{J}_3 = \begin{pmatrix} J_1 + 2J_{\pm\pm} \cos \frac{4\pi}{3} & 2J_{\pm\pm} \sin \frac{4\pi}{3} \\ 2J_{\pm\pm} \sin \frac{4\pi}{3} & J_1 - 2J_{\pm\pm} \cos \frac{4\pi}{3} \end{pmatrix}. \quad (7)$$

Using the auxiliary phases associated with the bond direction δ_α according to $\tilde{\varphi}_\alpha = \{0, -2\pi/3, 2\pi/3\}$ as in Refs. [2, 3], the two-site Hamiltonians in (4), (6), and (7) can be all reconciled as (minus the $J_{z\pm}$ term)

$$\hat{H} = J_1 \sum_{\langle ij \rangle} \left(\Delta S_i^{z_0} S_j^{z_0} + S_i^{x_0} S_j^{x_0} + S_i^{y_0} S_j^{y_0} \right) + 2J_{\pm\pm} \sum_{\langle ij \rangle} \left(S_i^{x_0} S_j^{x_0} - S_i^{y_0} S_j^{y_0} \right) \cos \tilde{\varphi}_\alpha - \left(S_i^{x_0} S_j^{y_0} + S_i^{y_0} S_j^{x_0} \right) \sin \tilde{\varphi}_\alpha. \quad (8)$$

Having in mind effects of disorder discussed below, we note that the variations of the diagonal elements of the exchange matrix (2) by $\pm \delta J_1$, translate into variations of $J_{\pm\pm}$ by $\pm \delta J_1/2$ (3), which can exceed its bare value.

$J_1 - J_2$ XXZ model

Given the hierarchy of terms in YbMgGaO₄ [1] ($J_{\pm\pm} \ll J_1$), we first neglect the pseudo-dipolar terms and consider the $J_1 - J_2$ XXZ model

$$\hat{H} = \sum_{\langle ij \rangle_n} J_n \left(\Delta S_i^{z_0} S_j^{z_0} + S_i^{x_0} S_j^{x_0} + S_i^{y_0} S_j^{y_0} \right) \quad (9)$$

where the sums are over the nearest- and next-nearest-neighbor bonds, $J_{1(2)} > 0$, same anisotropy $0 \leq \Delta \leq 1$ is assumed for both couplings, and $\{x_0, y_0, z_0\}$ is the laboratory reference frame, see Fig. 1. Triangular-lattice primitive vectors (in units of lattice spacing a) are $\delta_1 = (1, 0)$, and $\delta_{2(3)} = (\pm 1/2, \sqrt{3}/2)$. The next-nearest neighbor sites also form triangular lattices with the vectors $\delta_{1(3)}^{(2)} = (\pm 3/2, \sqrt{3}/2)$ and $\delta_2^{(2)} = (0, \sqrt{3})$.

Because of the XXZ anisotropy, the spins are in the x_0 - y_0 plane. Performing a standard rotation to the local

reference frames of individual spins and confining ourselves to the leading $1/S$ -order terms yields classical energy and harmonic SWT Hamiltonian. The two states compete for $0 < \alpha = J_2/J_1 < 1$, the 120° and the collinear (“stripe”) states, where in the latter rows of ferromagnetically ordered spins align antiferromagnetically, see Fig. 2. While the situation is somewhat more subtle for the selection of the stripe phase, see [6, 7], they suffice for our consideration. For the 120° state, J_2 couples spins on the same sublattices. For the stripe state, choosing the ferromagnetic rows in the x_0 -direction as in Fig. 2, only two of the J_2 bonds are ferromagnetic. The classical energies per site of the two states are

$$E_{\text{cl}}^{120^\circ}/S^2 = -3J_1/2 + 3J_2, \quad E_{\text{cl}}^{\text{coll}}/S^2 = -J_1 - J_2, \quad (10)$$

yielding a transition between the two at $\alpha_c = 1/8$, independently of Δ .

Linear spin-wave theory

In both phases, one obtains the harmonic Hamiltonian in a standard form

$$\hat{\mathcal{H}}^{(2)} = 3J_1S \sum_{\mathbf{k}} A_{\mathbf{k}} a_{\mathbf{k}}^\dagger a_{\mathbf{k}} - \frac{B_{\mathbf{k}}}{2} (a_{\mathbf{k}}^\dagger a_{-\mathbf{k}}^\dagger + \text{H.c.}), \quad (11)$$

with the Bogolyubov transformation giving magnon energy $\varepsilon_{\mathbf{k}} = 3J_1S\omega_{\mathbf{k}}$ with $\omega_{\mathbf{k}} = \sqrt{A_{\mathbf{k}}^2 - B_{\mathbf{k}}^2}$, and the ordered magnetic moment

$$\langle S \rangle = S - \frac{1}{2} \sum_{\mathbf{k}} \left(\frac{A_{\mathbf{k}}}{\omega_{\mathbf{k}}} - 1 \right). \quad (12)$$

Parameters for the 120° phase are

$$A_{\mathbf{k}} = 1 + (\Delta - 1/2) \gamma_{\mathbf{k}} - \alpha \left(2 - (\Delta + 1) \gamma_{\mathbf{k}}^{(2)} \right), \quad (13)$$

$$B_{\mathbf{k}} = -\gamma_{\mathbf{k}} (\Delta + 1/2) - \alpha (\Delta - 1) \gamma_{\mathbf{k}}^{(2)}, \quad (14)$$

and for the stripe phase

$$\bar{A}_{\mathbf{k}} = 2/3 + \Delta \gamma_{\mathbf{k}} + \gamma'_{\mathbf{k}} + \alpha \left(2/3 + \Delta \gamma_{\mathbf{k}}^{(2)} + \gamma'_{\mathbf{k}} \right), \quad (15)$$

$$\bar{B}_{\mathbf{k}} = \gamma'_{\mathbf{k}} - \Delta \gamma_{\mathbf{k}} + \alpha \left(\gamma_{\mathbf{k}}^{(2)} - \Delta \gamma_{\mathbf{k}} \right), \quad (16)$$

where we used the amplitudes

$$\gamma_{\mathbf{k}} [\gamma'_{\mathbf{k}}] = \frac{1}{3} \left(\cos k_x \pm 2 \cos \frac{k_x}{2} \cos \frac{\sqrt{3}k_y}{2} \right), \quad (17)$$

$$\gamma_{\mathbf{k}}^{(2)} [\gamma_{\mathbf{k}}^{\prime(2)}] = \frac{1}{3} \left(\cos \sqrt{3}k_y \pm 2 \cos \frac{3k_x}{2} \cos \frac{\sqrt{3}k_y}{2} \right).$$

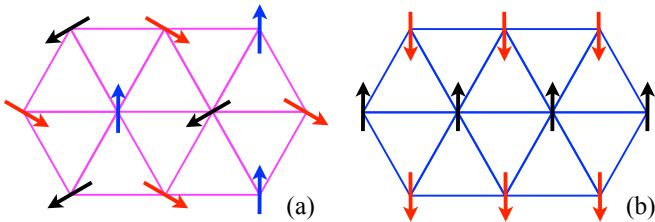


FIG. 2: (a) The 120° , and (b) the collinear (stripe) states.

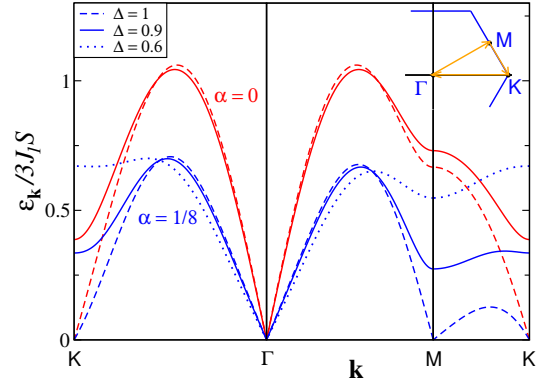


FIG. 3: $\omega_{\mathbf{k}}$ in the 120° phase for several α and Δ .

Magnon spectra

Since $\Delta < 1$ leaves only $U(1)$ symmetry intact, the spectra in both phases should exhibit only one Goldstone mode. This is the case for the 120° phase, see Fig. 3. At the Heisenberg limit ($\Delta = 1$), the Goldstone modes are at both Γ and $K(K')$ points [dashed lines] with an additional zero-mode occurring at the M points at the transition to the stripe phase, $\alpha = 1/8$. Since gaps grow with $1 - \Delta$, one can expect lower quantum fluctuations in the ground state and a more robust magnetic order for $\Delta < 1$.

The situation is more involved for the stripe phase where extra zero modes occur due to accidental degeneracy. The latter should be lifted by the fluctuations in the next order, see Refs. [6, 7]. In Fig. 4, we present $\omega_{\mathbf{k}}$ for the stripe state shown in Fig. 1, for which the ordering vector is M' with the mode at M points being accidental. Since the symmetry of the stripe state is different, the $\Gamma K M \Gamma$ and $\Gamma K' M' \Gamma$ directions are not equivalent.

One “dangerous” feature of the accidental zero modes is that the magnon dispersion near them for $\Delta = 1$ and any $\alpha > 1/8$ is $\omega_{\mathbf{k}} \propto k^2$. One can expect this to lead to logarithmically divergent fluctuation corrections [6], e.g., to the order parameter (12). However, we find that the fluctuation parts of the Bogolyubov transformation, $v_{\mathbf{k}}$, vanish along the $(k_x, \pm M'/2)$ lines that contain accidental zero modes, thus avoiding the divergence. Such vanishing of fluctuations is related to the ferromagnetic-like ordering along the x -direction. This feature allows us to stay within the linear SWT for the stripe state.

XXZ anisotropy gaps out zero modes at K, K' , and M' and modifies the dispersion of the accidental modes to a more standard $\omega_{\mathbf{k}} \propto k$. Overall, the trend is the same: $\Delta < 1$ reduces the role of quantum fluctuations and makes magnetic order more stable. In Fig. 4, we also plot the dispersion for $J_2/J_1 = 0.22$ and $\Delta = 0.58$ that are experimentally relevant to YbMgGaO_4 , [1].

XXZ phase diagram

From the character of the magnon spectra on both sides of the $\alpha = 1/8$ transition, one can see one important difference of the $J_1 - J_2$ problem on the triangular

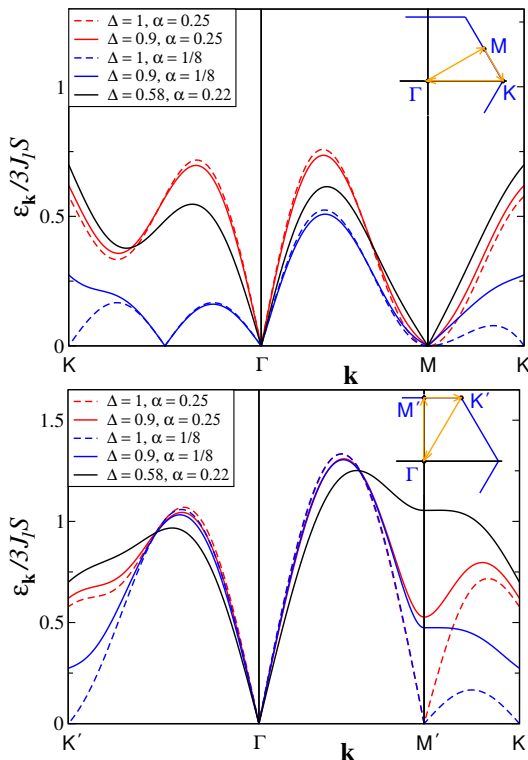


FIG. 4: $\omega_{\mathbf{k}}$ in the stripe phase for several α and Δ .

lattice from the square-lattice and other counterparts. Here, this transition is not associated with a divergence in the spin-wave fluctuation corrections. For instance, δS in (12) remains finite. This implies that at $S \gg 1$ the transition between the 120° and stripe phase must become a direct one for any Δ . In fact, within the SWT, the magnetically disordered state disappears already for $S=1$, in agreement with [8].

Another important feature of the problem, is that for $\Delta < 1$ the spectrum of the 120° state remains well-defined beyond the classical $\alpha_c = 1/8$ [8]. For $\Delta < 6/7$, it extends to $\tilde{\alpha}_c = 1/6$, and for $6/7 < \Delta < 1$ it is a straight line connecting α_c and $\tilde{\alpha}_c$, see Fig. 5. Thus, the stability regions of the spectra of the two phases always overlap for $\Delta < 1$, thus favoring a direct transition between them.

In Fig. 5 we present the SWT $\alpha - \Delta$ phase diagram of the XXZ model (9) for $S=1/2$. It is obtained from the α - and Δ -dependencies of the ordered moment (12), with their representatives shown in Fig. 6. The boundary of each phase is found from the $\langle S \rangle = 0$ condition. The direct transition between them is inferred from their magnetization crossings to signify the region where there is no intermediate non-magnetic state. The determination of such a transition from the crossings of the ground-state (GS) energies of the competing states meets rather standard difficulty within the SWT. Quantum corrections split the GS energies of the two phases, with no opportunity for a crossing in the region where both spectra are well-defined, see Fig. 5. However, one can still infer from Fig. 5 that the energy shift is more signifi-

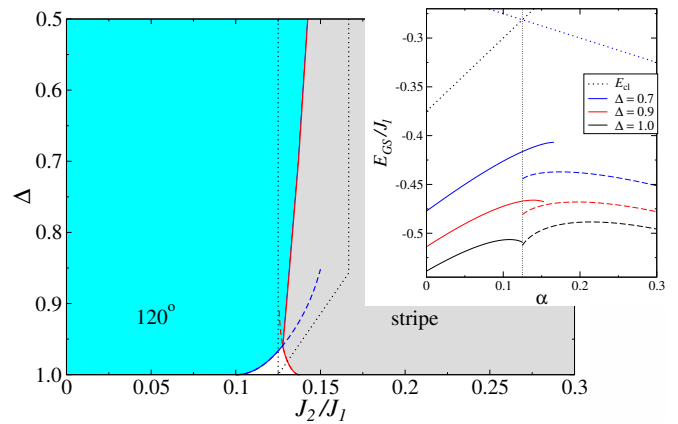


FIG. 5: Phase diagram Δ vs α . Right: E_{GS} vs α .

cant for the stripe phase, indicating that the transition is likely to shift toward smaller values of α for smaller Δ .

Thus, the XXZ anisotropy favors ordered states and, for the YbMgGaO_4 parameters ($J_2/J_1 = 0.22$ and $\Delta = 0.58$, see [1]), SWT places it in a stripe phase with a large ordered moment $\langle S \rangle \approx 0.32$, see orange dot in Fig. 6.

Pseudo-dipolar terms

The pseudo-dipolar terms are introduced in (8) and we omit the couplings of $S^{x_0(y_0)}$ to the out-of-plane spin components S^{z_0} , referred to as the $J_{z\pm}$ terms, as those are negligible in YbMgGaO_4 , see [1, 2].

For the spins in the coplanar configuration with the single ordering vector \mathbf{Q} , one can transform (8) to the local reference frames with the z -axes along the spin quantization axes and obtain the contribution of the pseudo-dipolar terms to the classical energy

$$\delta E_{cl} = J_{\pm\pm} S^2 \sum_{i,\pm\alpha} \cos(2\varphi_0 + 2\mathbf{Q} \cdot \mathbf{r}_i + \mathbf{Q} \cdot \boldsymbol{\delta}_{\pm\alpha} + \tilde{\varphi}_\alpha). \quad (18)$$

where $\tilde{\varphi}_\alpha$ is the auxiliary bond-dependent phase factor for the $\boldsymbol{\delta}_\alpha$ bonds, see Fig. 1, with $\tilde{\varphi}_\alpha = \{0, -2\pi/3, 2\pi/3\}$, $i \pm \alpha = \mathbf{r}_i \pm \boldsymbol{\delta}_\alpha$, and φ_0 is the spin direction relative to the x_0 axis at a reference site $i = 0$.

Stripe phase.—One can check whether the pseudo-dipolar terms favor deviations of the spins away from

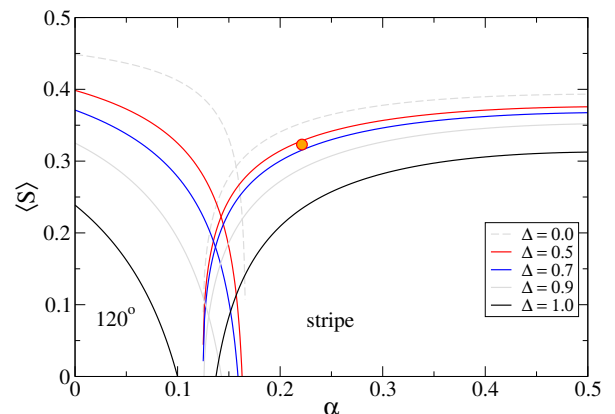


FIG. 6: $\langle S \rangle$ vs α .

the stripe order. This is done by considering $\hat{\mathcal{H}}_{p-d}$ in (8) and showing that the terms linear in the spin deviations vanish. Indeed, for any of the stripe states, on one of the bonds such linear terms vanish and the “tug” on the two other bonds cancels out. Thus, the pseudo-dipolar terms leave the stripe state stable.

One can see that $2\mathbf{Q} \cdot \mathbf{r}_i = 2\pi n$ for \mathbf{Q} at any of the M points (stripe ordering vectors). The $\mathbf{Q} \cdot \delta_{\pm\alpha}$ phase factors are either 0 or $\pm\pi$ for the three primitive vectors δ_α with their values dependent on the choice of \mathbf{Q} . That is, $\mathbf{Q} \cdot \delta_\alpha = \{\pi, \pi, 0\}$ for $\mathbf{Q} = M$, $\{0, \pi, \pi\}$ for $\mathbf{Q} = M'$, and $\{-\pi, 0, \pi\}$ for $\mathbf{Q} = M''$. Thus the classical energy contribution of the pseudo-dipolar terms simplifies to

$$\delta E_{cl} = 2J_{\pm\pm}S^2N \sum_{\alpha} \cos(2\varphi_0 + \mathbf{Q} \cdot \delta_\alpha + \tilde{\varphi}_\alpha). \quad (19)$$

Minimization of it with respect to the “global” spin angle φ_0 is expected to “pin” the orientation of the stripe spin structure in Fig. 2(b) to the lattice. Using the auxiliary phase factors $\tilde{\varphi}_\alpha$, one can find that the energy minimum is reached when the bonds $\delta_\alpha \perp \mathbf{Q}$ are satisfied completely ($\cos\theta_\alpha = -1$) while the other two bonds are partially satisfied ($\cos\theta_\alpha = -1/2$). This translates to the energy contribution $\delta E_{cl} = -4|J_{\pm\pm}|S^2N$ and the spins’ global orientation either parallel ($J_{\pm\pm} < 0$) or perpendicular ($J_{\pm\pm} > 0$) to the “happy” bond, depending on the sign of $J_{\pm\pm}$. To be specific, for the choice of $\mathbf{Q} = M'$ as in Fig. 2, the pseudo-dipolar terms will pin the spin orientation along the x_0 -axis (δ_1 bond) for $J_{\pm\pm} < 0$ and along the y_0 -axis if $J_{\pm\pm} > 0$, see Fig. 7.

For the contributions from the pseudo-dipolar terms to the magnon spectrum the sign of $J_{\pm\pm}$ does not matter as the choice of the “global” spin orientation angle φ_0 that minimizes energy also changes their overall sign to positive. Choosing $\mathbf{Q} = M'$ stripe order in accord with the choice above leads to the corrections to the spin-wave parameters in (6)

$$\delta\bar{A}_{\mathbf{k}} = \frac{8\eta}{3} + \frac{\eta}{2}(3\gamma_{\mathbf{k}} + \gamma'_{\mathbf{k}}), \quad \delta\bar{B}_{\mathbf{k}} = \frac{\eta}{2}(3\gamma_{\mathbf{k}} + \gamma'_{\mathbf{k}}), \quad (20)$$

where $\eta = |J_{\pm\pm}|/J_1$. Plots of the magnon energy $\varepsilon_{\mathbf{k}}$ along the $\Gamma MK\Gamma$ and the $\Gamma M'K'\Gamma$ cuts are shown in Fig. 8 for $\eta = 0.06$ and the same sets of parameters Δ and α as in Fig. 4. The most significant difference between Figs. 4 and 8 is the opening of sizable gaps and lifting of the accidental degeneracy mode at the M point. These effects are due to a low symmetry of the model with the

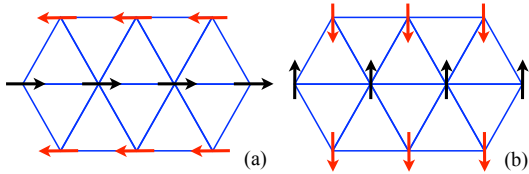


FIG. 7: Spin orientation in the stripe phase with $\mathbf{Q} = M'$ and pseudo-dipolar terms with (a) $J_{\pm\pm} < 0$ and (b) $J_{\pm\pm} > 0$.

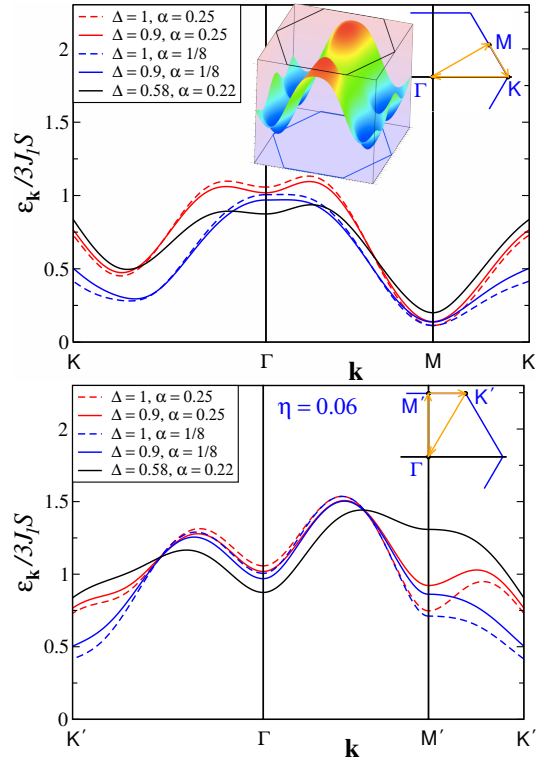


FIG. 8: $\omega_{\mathbf{k}}$ in the stripe phase for the same α and Δ as in Fig. 4, $\eta = |J_{\pm\pm}|/J_1 = 0.06$. Inset and black lines are the same.

pseudo-dipolar terms. This should strengthen the stripe order via a reduction of the quantum fluctuations.

120° state.—The consideration of the effects of the pseudo-dipolar terms on the 120° state is somewhat more involved. One can show that contributions of the three sublattices to the classical energy cancel each other and that the terms linear in spin deviations also vanish. Thus, the 120° state is locally stable to the pseudo-dipolar terms, $\delta E_{cl}^{120^\circ} = 0$, and no pinning of a particular global order parameter orientation to the lattice occurs.

Modified phase diagram

The most important outcome of the pseudo-dipolar terms is two-fold. First, the (per site) classical energy of the stripe state is lowered to $E_{cl}^{coll}/S^2 = -J_1 - J_2 - 4|J_{\pm\pm}|$ while the energy of the 120° state is unchanged from (10). This leads to an expansion of the stripe phase in the Δ - J_2 phase diagram with the classical transition moved down to $(J_2/J_1)_c = 1/8 - \eta$, completely suppressing the 120° state at a modest $|J_{\pm\pm}|/J_1 = 0.125$. Second, because of the lack of continuous symmetries, gapped excitation spectra should reduce quantum fluctuations and diminish the already suppressed magnetically disordered window of the anisotropic J_1 - J_2 XXZ model, making transition between the 120° and the stripe phase a direct one for the entire range of Δ at a rather small $J_{\pm\pm}$.

We demonstrate these effects in Fig. 9, which shows the α -dependence of the ordered moment for several Δ 's in the stripe phase. First set is the same as in Fig. 6

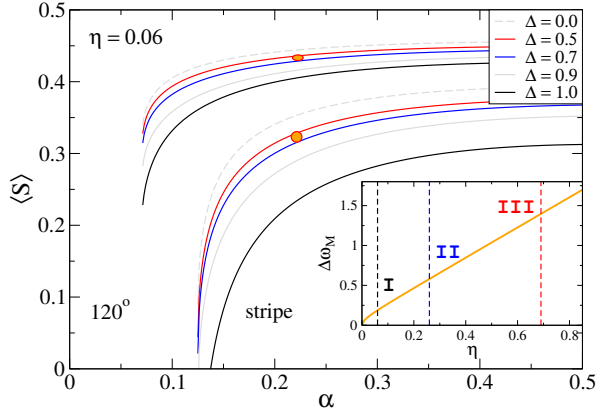


FIG. 9: $\langle S \rangle$ vs $\alpha = J_2/J_1$ for $\eta = |J_{\pm\pm}|/J_1 = 0$ and $\eta = 0.06$. Inset: lowest magnon gap in units of $3J_1S$ vs η by SWT.

for $J_1 - J_2$ XXZ model with $\eta = 0$ and the second is for $\eta = 0.06$. The orange dot marks $J_2/J_1 = 0.22$ and $\Delta = 0.58$ as before. It is clear that the stripe phase expands to the lower values of α and the ordered moment is increased, in agreement with the expectations. The transition in Fig. 9 is at the values only slightly larger than the classical value $\tilde{\alpha}_c = 0.065$ via an instability of the magnon branch at an incommensurate wavevector along the ΓK line.

Other parameter sets.—There are three sets of parameters that were inferred from the magnon dispersion of YbMgGaO_4 in the high-field phase. First is $\Delta = 0.58$, $\alpha = 0.22$, and $\eta = 0.06$ [1], which we use in our plots and will refer to as **Set I**. Second and third are attempts to fit the same data without next-neighbor exchange, so both have $\alpha = 0$ and $\Delta = 0.75$ and $\eta = 0.26$ [4] (**Set II**) and $\Delta = 0.55$ and $\eta = 0.69$ [1] (**Set III**), respectively.

We note that only **Set I** is compatible with the ESR data [2]. The values of $J_{\pm\pm}$ in **Sets II** and **III** put the system firmly in the stripe phase and have no 120° state in a vicinity. Moreover, **Sets II** and **III** correspond to much larger gaps in the magnon spectra than **Set I**, see inset in Fig. 9, which shows the lowest magnon energy vs η ; the SWT expression for the gap is given by $\Delta\omega_M = \frac{4}{3}\sqrt{2\eta(\eta + (1 - \Delta)/4)}$. While for YbMgGaO_4 **Set I** gives the gap ~ 0.06 meV, which is below experimental energy resolution [1], for both **Set II** and **Set III** the gaps are well above it and should have been readily observed. In addition, the values of the ordered moment within the SWT for all three sets are nearly classical: $\langle S \rangle = 0.433, 0.456, \text{ and } 0.486$, respectively.

Polarized phase, $H > H_s$, out-of-plane field

A strong out-of-plane magnetic field that is sufficient to co-align all the spins, should allow, at least in principle, to determine the magnitude of the pseudo-dipolar terms from several observables [1].

The full Hamiltonian is a combination of the $J_1 - J_2$ XXZ (9), the pseudo-dipolar from (8), and the field term $-h_z \sum_i S_i^{z0}$, where $h_z = g_z \mu_B \mu_0 H_z$ and g_z is the z -component of the anisotropic g -tensor. For the co-aligned

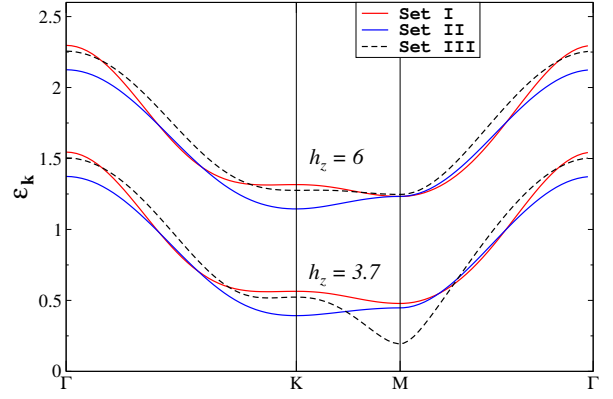


FIG. 10: $\epsilon_{\mathbf{k}}$ for YbMgGaO_4 ($3J_1S = 0.327$ meV) in the spin-polarized phase for two representative fields, $h_z/3J_1S = 6$ and 3.7 , and **Sets I, II, and III** [1, 4].

spins, they lead to a SWT Hamiltonian in a standard form (11) with the parameters

$$\begin{aligned} \tilde{A}_{\mathbf{k}} &= \frac{h_z}{3J_1S} - 2\Delta(1 + \alpha) + 2\gamma_{\mathbf{k}} + 2\alpha\gamma_{\mathbf{k}}^{(2)}, \\ \tilde{B}_{\mathbf{k}} &= \frac{4\eta}{3} \sum_{\alpha} e^{-i\tilde{\varphi}_{\alpha}} \cos k_{\alpha}, \end{aligned} \quad (21)$$

where $k_{\alpha} = \mathbf{k} \cdot \boldsymbol{\delta}_{\alpha}$ and $\omega_{\mathbf{k}} = \sqrt{\tilde{A}_{\mathbf{k}}^2 - \tilde{B}_{\mathbf{k}}^2}$ as before.

An important difference of the considered case from the more conventional models is that although the spins are co-aligned, the fluctuations are not zero even in the polarized state ($\tilde{B}_{\mathbf{k}} \neq 0$). Since fluctuations are only due to pseudo-dipolar terms, the latter can be determined, e. g., from the field-dependent behavior of the magnon dispersion. In the absence of fluctuations, high-field magnon dispersion would simply shift with the field. In Fig. 10 we present magnon dispersions for the two values of h_z and for the three sets of parameters discussed above.

The field of the transition from the stripe to the spin-polarized state also depends on the pseudo-dipolar terms. Since the gap at the M point vanishes at the transition, one finds $h_s = 6J_1S(\Delta + 1/3)(1 + \alpha) + 8|J_{\pm\pm}|S$. Since the magnetization is not fully saturated at $H > H_s$, it may be possible to extract $|J_{\pm\pm}|$ from its field dependence. Experiments in YbMgGaO_4 show M vs H that is surprisingly linear for $H < H_s$ without any clear cusp indicative of a transition. The lack of the upward curvature in $M(H)$ hints at the low role of quantum fluctuations, characteristic of the gapped phases.

Integrated intensity of $\mathcal{S}(\mathbf{q}, \omega)$.—Yet another measurable quantity is the ω -integrated dynamical structure factor $\mathcal{S}(\mathbf{q}, \omega)$. In a fully polarized state, which is in a way identical to a ferromagnetic state, integration over the sharply-defined single-magnon sector yields a function that is independent of \mathbf{q} . This is precisely because of the absence of quantum fluctuations in the fully saturated phase. In our case, the fluctuations are present and $\mathcal{S}(\mathbf{q})$ will be modulated in \mathbf{q} . The modulation is directly proportional to the strength of the pseudo-dipolar terms.

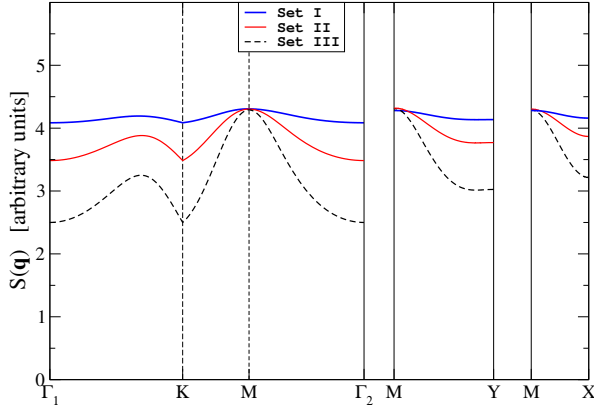


FIG. 11: $\mathcal{S}(\mathbf{q})$ for the same Sets as in Fig. 10, $h_z/3J_1S=5.2$.

While this modulation may not be easily detectable for small $J_{\pm\pm}$, such as in the Set I, the lack of a significant modulation can help ruling out larger values of the pseudo-dipolar terms.

The in-plane component of the structure factor can be obtained as

$$\mathcal{S}(\mathbf{q}) = \frac{S}{2} \left(\frac{\tilde{A}_{\mathbf{q}}}{\omega_{\mathbf{q}}} + \frac{(q_y^2 - q_x^2)\text{Re}\tilde{B}_{\mathbf{q}} - 2q_xq_y\text{Im}\tilde{B}_{\mathbf{q}}}{q^2\omega_{\mathbf{q}}} \right), \quad (22)$$

with $\tilde{A}_{\mathbf{q}}$ and $\tilde{B}_{\mathbf{q}}$ from (21).

Our Fig. 11 shows the \mathbf{q} -modulation of $\mathcal{S}(\mathbf{q})$ for the three sets of parameters discussed above. It is important to note that the momentum dependence of the ω -integrated structure factor $\mathcal{S}(\mathbf{q})$ is different in the first and the subsequent Brillouin zones because of the explicit \mathbf{q} -dependence in the fluctuation-induced terms in (22). This observation offers a yet another potential avenue of determining the values of the pseudo-dipolar terms.

Details of the DMRG calculations

For the DMRG calculations in the 6×36 cylinders, we perform 24 sweeps and keep up to $m = 2000$ states with truncation error less than 10^{-5} . For the 6×12 cylinders, we perform 32 sweeps and keep up to $m = 2000$ states with truncation errors less than 10^{-6} . In the real-space images of cylinders, the size of the arrows represent the measurement of local spin with the directions of the spins in the xy plane. The width of the bond on the lattice represents the nearest-neighbor spin-spin correlation, with ferromagnetic correlation shown as dashed and antiferromagnetic ones as solid lines.

In Fig. 12, we provide a more detailed exposition of the long-cylinder DMRG “scans” of the XXZ model (9) and of the same model with the $J_{\pm\pm}$ terms from (8). The calculations are done on 6×36 cylinders at fixed Δ 's and $J_{\pm\pm}$. The J_2 is varied between 0 and $0.25J_1$ along the length of the cylinder. The orders, which are verified to exist at the limiting J_2 values, are pinned at the boundaries. The boundaries of the long cylinders are at $J_2 = 0$, where the stability of the 120° state is well established, or at a rather large J_2 where the stripe state

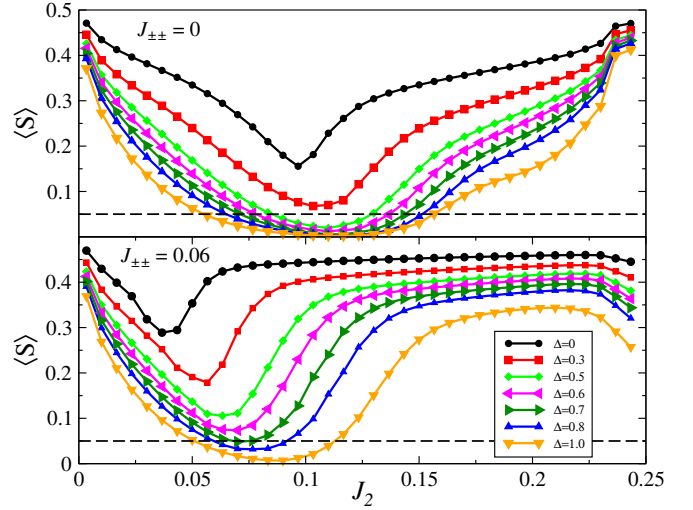


FIG. 12: The long-cylinder DMRG scans of $\langle S \rangle$ vs J_2 for various Δ 's and $J_{\pm\pm} = 0$ and $J_{\pm\pm} = 0.06J_1$.

is also well known to be stable. We have also performed “narrowing” of the window of the scan (range of J_2), to reduce the gradient of its change in order to verify the stability of our results and the lack of induced-order effect. Fig. 12 shows the profiles of the ordered moments $\langle S \rangle$ vs J_2 for several Δ 's and for $J_{\pm\pm} = 0$ and $J_{\pm\pm} = 0.06J_1$. We estimated that in our clusters, $\langle S \rangle = 0.05$ line should separate the cases of a direct transition between the 120° and the stripe phase from the ones where it goes through an intermediate non-magnetic state. This yields a criterion for the spin-liquid (SL) boundaries and it matches such boundaries for the Heisenberg $J_1 - J_2$ model [9].

We use scans in Fig. 12 to provide estimates for the SL boundaries, with more careful verifications usually conducted on shorter 6×12 cylinders for fixed values of J_2 via correlation functions and by studying decay of spin correlations away from the edges with induced orders [9]. For instance, several points within the “spin-liquid domes” of the phase diagram in Fig. 1 of the main text have been checked to verify that the state is indeed magnetically disordered and that the correlation length of any induced order, either by pinning a spin with a field in the center or at the boundaries, falls off exponentially.

One can see for the $J_{\pm\pm} = 0.06J_1$ case, that the order is strengthened and the non-magnetic region shrinks considerably. We estimate that $J_{\pm\pm} \approx 0.1J_1$ is sufficient to eliminate the SL state completely.

Disorder.—As noted above, according to the parametrization introduced in (3), $J_{\pm\pm} = (J_{xx} - J_{yy})/4$, the variations of the diagonal elements J_{xx} and J_{yy} of the exchange matrix in (2) by δJ_1 translate into variations of $J_{\pm\pm}$ by $\delta J_1/2$. If $J_{xx} \approx J_{yy}$, which is the case of YbMgGaO_4 , the bare value of $J_{\pm\pm}$ is small and variations of the exchange matrix of order 20% suggested in [10], imply a spatial distribution of completely random pseudo-dipolar $J_{\pm\pm}$ bonds of different sign.

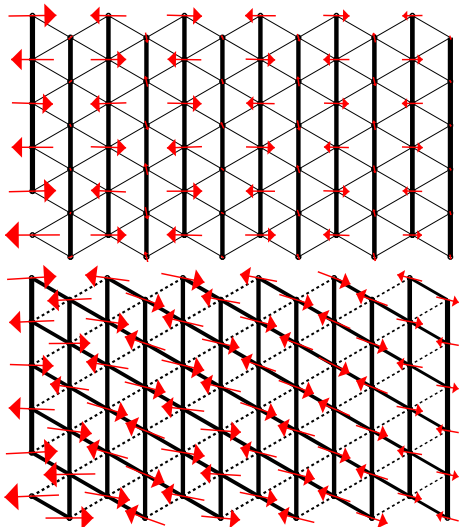


FIG. 13: The 6×12 DMRG cylinder, $J_2 = 0.22J_1$, $\Delta = 0.58$, and random $J_{\pm\pm} = \pm 0.05J_1$ with one [upper image] or two [lower image] spins at the lower left edge pinned by the field in the horizontal direction.

In our DMRG simulations of the XXZ model we use binary distributions of $J_{\pm\pm}$ of alternating sign on a 6×12 clusters. All presented results are from individual disorder realizations. They are all relatively time consuming to run and to extract spin correlations. The final figures for the static structure factor (Fig. 4(d) of the main text and Fig. 14(b) below) included the averaging over orientations to help restore the full orientational symmetry of the lattice that was affected by the boundaries.

We find that for smaller values of $|J_{\pm\pm}| = 0.05J_1$ and $0.1J_1$, not only an effective $U(1)$ symmetry of the XXZ model is recovered (real-space order is not pinned to the lattice), but also the Z_3 lattice symmetry, broken in each individual stripe state, is effectively restored due to a randomization of $J_{\pm\pm}$. This is demonstrated by the structure factor showing broadened peaks at two different M-points associated with two different stripe orderings, with the third stripe direction strongly suppressed by the cluster geometry, see main text. We refer to these states as to the *stripe-superposition* states, in which stripe orders coexist in a fluctuating manner.

The details of this unusual state are revealed by probing it with various pinning fields. In the first one, one spin is pinned at the edge (lower left corner), see Fig. 13. The resulting pattern over the whole cluster is associated with an almost equal superposition of the two types of stripes, with M and M'' ordering vectors, running across each other. In this case, the structure factor continues to show two peaks at these two M-points even with the strong pinning field. In the second such experiment, we apply a pinning field to a second site in the next column in order to favor one of the stripe orders, see Fig. 13. That state is indeed revealed, the single-stripe real-space

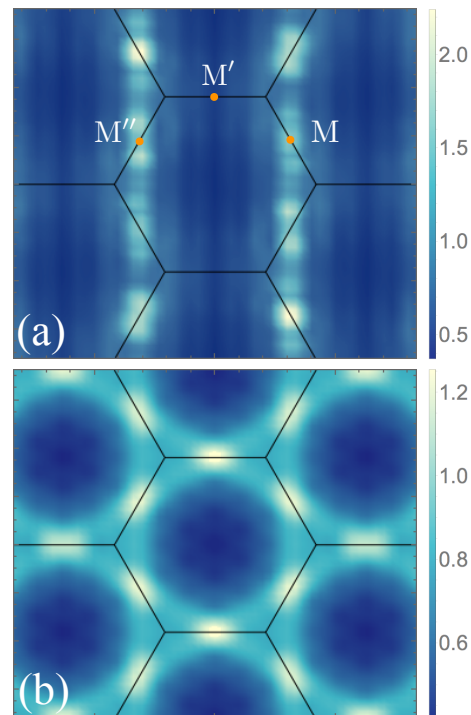


FIG. 14: (a) Structure factor $S(\mathbf{q})$ for a domain-like disordered state for random $J_{\pm\pm} = \pm 0.2J_1$. (b) Same, averaged to restore the suppressed stripe direction.

ordered pattern emerges, and the second peak in $S(\mathbf{q})$ becomes suppressed when the pinning field is made strong.

For smaller $J_{\pm\pm}$ and for most disorder realizations, we found stripe-superposition states, and for some other realizations the state was a robust stripe state of one orientation. This is consistent with most disorder distributions allowing fluctuations between the stripes to exist within the domains of the size of our clusters, and for the other distributions, which for some reason are more biased, disorder is pinning one stripe orientation domain.

For larger values of the randomized $J_{\pm\pm} = \pm 0.2J_1$, we found disordered spin domains with mixed stripe orientations forming static structures with large ordered moments, see main text. Here we show the associated structure factor, see Fig. 14. For larger random $J_{\pm\pm} = \pm 0.2$, the correlation length becomes compatible with the cluster size, and we have observed either robust stripes or a coexistence of the stripe domains within a cluster, as shown in our Fig. 4(b) of the main text. The shorter stripe domain sizes at stronger disorder (correlation length ~ 6 lattice sites for $J_{\pm\pm} = \pm 0.2$) is consistent with a general expectation.

In the last Figure 15, we compare 1D cuts of the orientationally-averaged structure factor $S(\mathbf{q})$ for the stripe-superposition states for smaller random $J_{\pm\pm} = \pm 0.05J_1$ and $\pm 0.1J_1$ from the main text with the glass-like $S(\mathbf{q})$ for larger $J_{\pm\pm} = \pm 0.2J_1$ in Fig. 14. Both cases, the glass-like mixed-stripe and the stripe-superposition

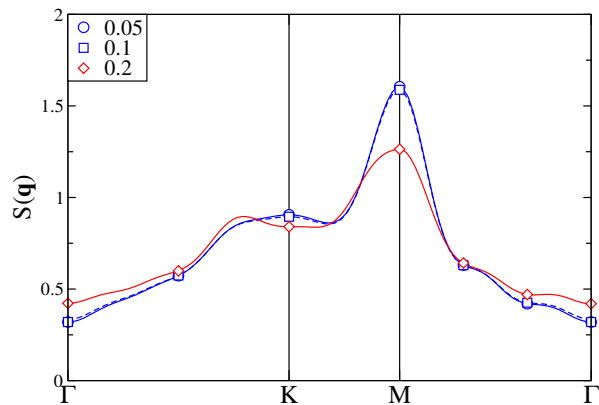


FIG. 15: 1D cuts of the averaged structure factor $S(\mathbf{q})$.

states, result in the $S(\mathbf{q})$ structure that is strongly reminiscent of the experimental results in YbMgGaO_4 [1].

Note on the $J_{z\pm}$ terms.—We have performed some preliminary DMRG calculations [11] of the J_1 -only XXZ model with the so-called $J_{z\pm}$ terms [2, 3], see (4), which were initially dropped in the context of YbMgGaO_4 as they were found to be small [2]. These calculations show a direct transition between robust 120° and stripe phases at rather large $J_{z\pm} \approx 0.3J_1$ with no indication of a spin-liquid away from the Heisenberg limit of the XXZ term.

-
- [1] J. A. M. Paddison, M. Daum, Z. Dun, G. Ehlers, Y. Liu, M. B. Stone, H. Zhou, and M. Mourigal, *Nat. Phys.* **13**, 117 (2017).
 - [2] Y. Li, G. Chen, W. Tong, Li Pi, J. Liu, Z. Yang, X. Wang, and Q. Zhang, *Phys. Rev. Lett.* **115**, 167203 (2015).
 - [3] Y. Shen, Y.-D. Li, H. Wo, Y. Li, S. Shen, B. Pan, Q. Wang, H. C. Walker, P. Steffens, M. Boehm, Y. Hao, D. L. Quintero-Castro, L. W. Harriger, M. D. Frontzek, L. Hao, S. Meng, Q. Zhang, G. Chen, and J. Zhao, *Nature* **540**, 559 (2016).
 - [4] Y.-D. Li, Y. Shen, Y. Li, J. Zhao, and G. Chen, arXiv:1608.06445.
 - [5] M. E. Zhitomirsky, M. V. Gvozdkova, P. C. W. Holdsworth, and R. Moessner, *Phys. Rev. Lett.* **109**, 077204 (2012).
 - [6] A. V. Chubukov and Th. Jolicoeur, *Phys. Rev. B* **46**, 11137 (1992).
 - [7] Th. Jolicoeur, E. Dagotto, E. Gagliano, and S. Bacci, *Phys. Rev. B* **42**, 4800(R) (1990).
 - [8] N. B. Ivanov, *Phys. Rev. B* **47**, 9105 (1993).
 - [9] Z. Zhu and S. R. White, *Phys. Rev. B* **92**, 041105 (2015).
 - [10] Y. Li, D. Adroja, R. I. Bewley, D. Voneshen, A. A. Tsirlin, P. Gegenwart, and Q. Zhang, arXiv:1702.01981.
 - [11] Z. Zhu *et al.*, unpublished.